INTER-NOISE 2007
28-31 AUGUST 2007
ISTANBUL, TURKEY

Nonlinear median transform domain denoising of frequency response functions

Berke M. Gur[a] and Christopher Niezrecki[b]
University of Massachusetts – Lowell
Department of Mechanical Engineering
Structural Dynamics and Acoustic Systems Laboratory
One University Ave., Lowell, MA 01854
USA

ABSTRACT

Frequency response functions (FRF) are the primary means of experimentally evaluating the structural characteristics of vibrating systems. Vibration analyzers estimate the FRF through the ratio of the output/input power spectral densities (PSD); which in turn are estimated using periodograms. However, periodograms are inconsistent estimators. In addition, noise in the input and output data further degrade the performance of the periodogram. Therefore, practical estimation of FRFs from noisy measurements is achieved through time averaged periodograms. In the last decade, the discrete wavelet transform (DWT) has emerged as a powerful tool for denoising functions. Recently, wavelet domain post processing methods have been suggested to eliminate noise contamination in FRFs, as an alternative to time averaging. The Median Interpolating Pyramid transform (MIPT) based denoising algorithm is inherently similar to DWT algorithms. However, it is more capable of eliminating impulsive noise and is an alternate method for improving FRF estimates. In this work, a MIPT based denoising algorithm is implemented to eliminate impulsive and Gaussian noise contamination of FRF estimates. Preliminary results obtained using simple 2 degree-of-freedom (DOF) systems demonstrate that an average improvement of 5 dB can be achieved using the MIPT algorithm as a post processor to the traditional periodogram based estimate.

1 INTRODUCTION

FRFs are the primary means for characterizing structural properties of vibrating linear, time invariant (LTI) systems and play a central role in experimental mechanics. In particular, accurate estimates of FRFs are vital for modal analysis, structural modification, system identification, etc. [1]. Their popularity stems from the fact that they can be efficiently measured from experimental data through FFT based periodogram estimation. Some practical difficulties related to periodogram estimation are the inconsistency of the periodogram and the high sensitivity of the FRFs to measurement errors made in the input and output of the system. The most popular method of reducing estimation variance and noise contamination in periodograms is to compute a time averaged periodogram [2], [3]. The required number of time averages, and thus measurement interval, increases as measurement noise becomes more significant. This increased sampling interval not only increases the computational load, but can also result in the violation of the LTI system assumption. An alternate to time averaging is to post process the periodograms using some noise reduction scheme.

[a] Email address: berke_gur@student.uml.edu
[b] Email address: christopher_niezrecki@uml.edu

Although the wavelet transform was initially developed for time-frequency analysis as an alternative to the short time Fourier transform (STFT), it has found several other important application areas. One such application is wavelet domain noise reduction [4] which has been successfully applied in many disciplines such as audio and medical image restoration, communications, time series analysis and forecasting, etc. [5]. The flexibility and noise reduction performance of wavelet transform based methods make them suitable candidates for FRF noise reduction. Bodin and Wahlberg assumed identically and independently distributed (i.i.d.) Gaussian measurement noise at the output only and analyzed wavelet coefficient shrinkage denoising of FRFs obtained through Blackman-Tukey PSD estimates using a Hanning window [6]. While wavelet domain denoising methods are effective in eliminating Gaussian noise, their denoising performance suffers if the noise is heavy tailed. When measurement errors are made in both the outputs and inputs, the resulting FRF is contaminated with impulsive noise. Kim *et al*. pointed to this impulsive noise in FRF estimates and suggested denoising FRFs through a combination of median filtering and wavelet denoising [7]. The method implemented in Reference 7 was proposed by Bruce *et al*. [8] to improve the denoising performance of wavelet coefficient shrinkage algorithms in the presence of impulsive noise. In this paper, the MIPT based coefficient shrinkage algorithm, developed by Donoho and Yu [9], [10], is proposed for post processing of noisy FRFs. The method implemented does not utilize the wavelet transform, yet it is very similar and shares several concepts related to wavelet coefficient shrinkage denoising; and heavily utilizes medians. The noise reduction method proposed in this paper provides researchers and engineers with an alternate tool for denoising FRFs, with the possibility of reducing the number of time averages required to obtain consistent FRF estimates.

2 THEORY

2.1 Classical Spectral FRF Estimation

The input-output relationship of a LTI system is given through the convolution integral:

$$y(t) = \int_{-\infty}^{\infty} h(t-\tau)u(\tau)d\tau, \tag{1}$$

where $y(t)$, $u(t)$, and $h(t)$ are the output, input, and system impulse response, respectively. The true FRF of the system, $H(f)$ is defined as the Fourier transform of the system impulse response. The FRF is calculated as the ratio of the cross- and auto-PSD of the output and input:

$$H(f) = \frac{P_{xy}(f)}{P_{xx}(f)}. \tag{2}$$

The PSD is defined as:

$$P_{xx}(f) = \lim_{M\to\infty} E\left\{\frac{1}{2M+1}\left|\sum_{n=-M}^{M} x(n)\exp(-j2\pi fn)\right|^2\right\}, \tag{3}$$

where $E(\cdot)$ represents the expectation operator. For practical purposes, the expectation operator in Eq. (3) is neglected and the PSD is estimated very efficiently using the periodogram:

$$\hat{P}_{xx}(f) = \frac{1}{N}\left|\sum_{n=0}^{N-1} x(n)\exp(-j2\pi fn)\right|^2, \tag{4}$$

where N samples are used for the estimate. It can be shown that the periodogram is asymptotically unbiased:

$$\lim_{N\to\infty} E[\hat{P}_{xx}(f)] = P_{xx}(f). \tag{5}$$

However, the periodogram is also an inconsistent estimator with its variance independent of the number of samples used in the estimate:

$$\text{var}[\hat{P}_{xx}(f)] \approx P_{xx}^2(f). \tag{6}$$

From Eqs. (5)-(6), it is observed that the uncertainty associated with the periodogram estimates is of the order of the estimate itself, indicating a poor estimator performance. This inconsistency and poor performance of the periodogram is attributed to elimination of the expectation operator in going from Eq. (3) to Eq. (4). In an effort to reduce the variance of the periodogram, the Welch periodogram divides the available N data samples into K, possibly overlapping, clusters, each with L samples, and the PSD is estimated through averaging the K periodograms, each obtained using L data samples. For non-overlapping data samples, the variance of the periodogram reduces to [3]:

$$\text{var}[\hat{P}_{xx,aver}(f)] \approx \frac{1}{K}\text{var}\left[\sum_{m=0}^{K-1} P_{xx}^{(m)}(f)\right]. \tag{7}$$

The data can be windowed prior to the peridogram estimate to reduce sidelobes in case of narrowband signals. The ensemble averaging of the PSD in Eq. (3) is replaced with the time averaging in Eq. (7). Time averaging results in a conflict between unbiased and consistent estimation of the PSD. That is, for a given number of samples N, dividing these samples into more clusters with fewer samples reduces the variance of the PSD estimates. However, since the PSD is only asymptotically unbiased, this can increase the bias of each of the K periodogram estimates.

2.2 Effects of Measurement Noise on FRF Estimates

Aside from inconsistent PSD estimates, FRFs are also affected by measurement noise at the input and outputs. In the presence of measurement noise, the convolution integral becomes:

$$z(t) = \int_{-\infty}^{\infty} h(t-\tau)x(\tau)d\tau + v(t), \tag{8}$$

where $x(t) = u(t) + w(t)$ is the noisy input signal. While modeling measurement noise as a Gaussian process [i.e., $v(t) \sim \mathcal{N}(0,\sigma_v^2)$; $w(t) \sim \mathcal{N}(0,\sigma_w^2)$] is a reasonable assumption, the resulting noise in the FRFs is highly impulsive and cannot be modeled as additive Gaussian noise. Based on previous results reported in the literature [7] and empirical observations, FRF noise is modeled as non-Gaussian, impulsive noise. In particular, the symmetric alpha stable (SαS) distribution is a viable candidate for modeling FRF noise. Furthermore, both the Gaussian and the heavier tailed Cauchy distributions are special cases of SαS distributions [11]. Under the SαS noise assumption, the noisy FRF is represented as:

$$Z(f) = H(f) + N(f), \tag{9}$$

where $Z(f)$ is the noisy FRF, $H(f)$ represents the true FRF, and $N(f)$ represents heavy tailed noise contamination. Without the loss of generality, normalized frequencies are assumed such that $0 \le f < 1$.

2.3 Wavelet Domain Noise Reduction

The discrete wavelet transform (DWT) of the FRF is defined as the integral transform:

$$\{\mathcal{W}Z\}(j,k) = \int_0^1 Z(\xi) 2^{-j/2} \psi(2^{-j}\xi - k) d\xi, \tag{10}$$

where $\psi(\xi)$, j and k are the wavelet basis function, scale and translation variables, respectively. For various values of the scale variable, the DWT decomposes the function into coefficients representing the characteristics of the function at different resolutions. The output of this transform is a vector of approximate and detail coefficients, which carry low and high frequency information about the function, respectively. The classical wavelet domain noise reduction algorithms perform nonlinear thresholding on the detail wavelet coefficients of the noisy signal. The noise free signal is obtained through an inverse DWT of the thresholded coefficients. The fundamental idea behind wavelet domain noise reduction is that the function is mapped to a few coefficients with large magnitudes while noise is spread over the entire range of translations as small amplitude coefficients. This mapping is very effective when noise is Gaussian and it has been shown that classical wavelet domain denoising methods achieve near asymptotic minimax performance for functions of certain smoothness classes [4]. However, these methods breakdown when noise contamination is much more impulsive compared to Gaussian noise, as coefficients due to impulsive noise get mapped as high amplitude coefficients and elude thresholding.

2.4 Robust Wavelet Denoising

Robust wavelet denoising (RWD) was developed to improve the noise reduction performance of wavelet domain algorithms in case of impulsive noise [8]. The RWD is similar to DWT based algorithms except for a median filtering stage imposed on approximate coefficients. The approximate coefficients, to which impulsive noise is likely to leak, is subtracted from their median. If the coefficient is due to impulsive noise, then this difference will be large. Therefore, a soft threshold is applied to this difference between the coefficients and the median. As a result of this threshold, the impulsive noise coefficients are likely to pass unaffected. Subtracting these thresholded differences from the actual approximate coefficients eliminates impulsive noise components, for an appropriate selection of the threshold. The detail coefficients are thresholded as in the case of the DWT to eliminate Gaussian noise. Thus, the RWD is capable of eliminating both impulsive noise and Gaussian noise, through median filtering and classical wavelet thresholding, respectively.

2.5 Median Interpolating Pyramid Transform Thresholding

The median interpolating pyramid transform (MIPT) based denoising method developed by Donoho and Yu [10] is very similar to both the DWT and RWD algorithms. Its similarity to the DWT algorithm lies in the fact that it involves three stages. The forward transform maps the signal to the transform domain, followed by a thresholding operation to eliminate the coefficients due to noise. The noise-free signal is recovered through an inverse MIPT. On the other hand, it utilizes medians to eliminate impulsive noise, similar to the RWD algorithm. In the MIPT, the number of spectral lines is assumed to be a triadic number

$N = 3^J$ such that $0 \le f \le (1 - 3^{-J})$. The MIPT maps the data to the transform domain by constructing triadic groups of signal samples at a given scale and computing their median:

$$m_{j,k} = \text{median}[Z(f)], \quad f \in I_{j,k} = [k \cdot 3^{-j}, (k+1) \cdot 3^{-j}), \tag{11}$$

where $j \ge 0$ is a non-negative integer representing the scale variable; $0 \le k < 3^j$ is the non-negative integer representing translation variable. In the core of the MIPT is a set of quadratic interpolating polynomials $\pi_{j,k}(f) = a_{j,k} + b_{j,k} f + c_{j,k} f^2$, defined for each interval, $I_{j,k}$, with a median matching the median of the noisy function at the corresponding scale around a triadic group of translations centered at k:

$$\begin{aligned} &\text{median}[\pi_{j,k}(f)] = m_{j,k-1}, \quad f \in I_{j,k-1}, \\ &\text{median}[\pi_{j,k}(f)] = m_{j,k}, \quad f \in I_{j,k}, \\ &\text{median}[\pi_{j,k}(f)] = m_{j,k+1}, \quad f \in I_{j,k+1}. \end{aligned} \tag{12}$$

It is shown in Reference 10 that the coefficients $(a_{j,k}, b_{j,k}, c_{j,k})$ of the quadratic interpolating polynomial for an arbitrary set of medians $(m_{j,k-1}, m_{j,k}, m_{j,k+1})$ are unique and can be obtained analytically. This set of polynomials $\pi_{j,k}$ is in turn used to estimate the medians of the triadic group of coefficients at the next higher resolution scale:

$$\begin{aligned} \tilde{m}_{j+1,3k} &= \text{median}[\pi_{j,k}(f)], \quad f \in I_{j,3k}, \\ \tilde{m}_{j+1,3k+1} &= \text{median}[\pi_{j,k}(f)], \quad f \in I_{j,3k+1}, \\ \tilde{m}_{j+1,3k+2} &= \text{median}[\pi_{j,k}(f)], \quad f \in I_{j,3k+2}. \end{aligned} \tag{13}$$

Similar to the last stage of the median filtering of the RWD algorithm, the difference between the actual medians $m_{j,k}$ and the estimates $\tilde{m}_{j,k}$ obtained through the polynomial $\pi_{j,k}$ is said to be the transform coefficients $\alpha_{j,k}$ at a given scale j and translation k:

$$\alpha_{j,k} = m_{j,k} - \tilde{m}_{j,k}. \tag{14}$$

This polynomial construction, median estimation and coefficient calculation sequence is repeated until a predefined cut-off scale j_0 is reached. The coefficients at this final terminal scale j_0 are set to the medians for this scale (i.e., $m_{j_0,k}$). The MIPT results in a vector of coefficients:

$$\boldsymbol{\theta} = [\mathbf{m}_{j_0}^T \quad \boldsymbol{\alpha}_{j_0+1}^T \quad \cdots \quad \boldsymbol{\alpha}_J^T]^T, \tag{15}$$

where $\mathbf{m}_{j_0}(k) = m_{j_0,k}, \quad 0 \le k < 3^{j_0}$ and $\boldsymbol{\alpha}_j(k) = \alpha_{j,k}, \quad 0 \le k < 3^j$.

Following MIPT decomposition, a hard threshold is imposed on the normalized coefficients $\bar{\alpha}_{j,k} = 3^{(J-j)/2} \alpha_{j,k}$:

$$\delta_\eta^h(\bar{\alpha}_{j,k}) = \begin{cases} \bar{\alpha}_{j,k}, & |\bar{\alpha}_{j,k}| \ge \eta_j, \\ 0, & |\bar{\alpha}_{j,k}| < \eta_j, \end{cases} \tag{16}$$

where $\boldsymbol{\eta} = [\eta_{j_0+1} \quad \eta_{j_0+2} \quad \cdots \quad \eta_J]^T$ is a vector of scale dependent thresholds. The MIPT based denoising algorithm assumes that the coefficients $\alpha_{j,k}$ below a given threshold are due to noise and their elimination from the reconstruction process results in denoising. The thresholds are determined through asymptotic properties of random variables. In particular, it is desirable to find a threshold η_j such that the probability of the MIPT coefficients due to i.i.d. noise exceeding this threshold asymptotically approaches zero:

$$\lim_{N\to\infty} \Pr(|\bar{\alpha}_{j,k}| > \eta_j) \to 0. \tag{17}$$

When noise can be characterized through a symmetric probability distribution $F_v(v)$, this threshold is shown to be:

$$\eta_j = 3^{(J-j)/2} F_v^{-1}(\xi), \quad \xi = 1/2 + \left[1 - (2J3^J)^{-2/(3^{J-j})}\right]^{1/2}/2. \tag{18}$$

Most SαS distributions do not possess an analytic distribution function, and Eq. (18) cannot be solved explicitly to obtain a threshold. However, the contribution of the distribution to the threshold does not vary significantly at the course scales for different SαS distributions. Therefore, the thresholds for a SαS noise distribution can be estimated through the thresholds for SαS distributions that possess analytical distribution functions. Gaussian or Cauchy distributions are suitable candidates for this purpose.

After elimination of the coefficients due to noise through hard thresholding, the noise free estimate of the function is obtained by reconstruction of the remaining coefficients through the inverse MIPT. Detailed discussions related to the MIPT, the inverse MIPT, the properties and implementation of the MIPT and the thresholds can be found in Reference 10.

3 SIMULATION RESULTS AND DISCUSSIONS

The MIPT based denoising scheme is implemented on a hypothetical multi-input, multi-output (MIMO) system defined by:

$$\begin{aligned} \ddot{x}_1(t) + 100\dot{x}_1(t) + 428400x_1(t) - 132900x_2(t) &= u_1(t), \\ \ddot{x}_2(t) + 100\dot{x}_2(t) - 132900x_1(t) + 428400x_2(t) &= u_2(t), \end{aligned} \tag{19}$$

where $u_i(t),\ x_i(t),\ i = 1,2$ are the system inputs and outputs, respectively. The transfer function of this MIMO system is:

$$\mathbf{G}(s) = \frac{\begin{bmatrix} G_{11}(s) & G_{12}(s) \\ G_{21}(s) & G_{22}(s) \end{bmatrix}}{(s + 50 \pm j579.06)(s + 50 \pm j787.96)}, \tag{20}$$

where

$$\begin{aligned} G_{11}(s) &= s^2 + 100s + 532800, & G_{12}(s) &= 132900, \\ G_{21}(s) &= 132900, & G_{22}(s) &= s^2 + 100s + 428400. \end{aligned} \tag{21}$$

The system input and outputs are sampled at a rate of 400 Hz. The system magnitude FRF $H_{12}(f)$ between output $X_1(f)$ and input $U_2(f)$ is analytically calculated and plotted in figure 1. Also plotted in figure 1 is a single periodogram estimate using 4372 noisy input and

output samples (input SNR = 20 dB, output SNR = 35 dB) demonstrating the impulsive noise contamination on the FRF. The estimation and denoising performance of analyzed algorithms are evaluated through the SNR measure defined as:

$$\mathrm{SNR}(Z) = 10 \cdot \log_{10} \left\{ \frac{\frac{1}{N} \sum_{f=0}^{1-3^J} [H(f)]^2}{\frac{1}{N} \sum_{f=0}^{1-3^J} [Z(f) - H(f)]^2} \right\}. \tag{22}$$

The SNR of the periodogram in figure 1 is calculated to be 13.8 dB. MIPT based denoising is applied to this single PSD estimate with a maximum scale of $J = 7$ and a cutoff scale of $j_0 = 4$. The MIPT denoised result is plotted along with the true FRF in figure 2. Following MIPT denoising, the SNR increases to 18.7 dB.

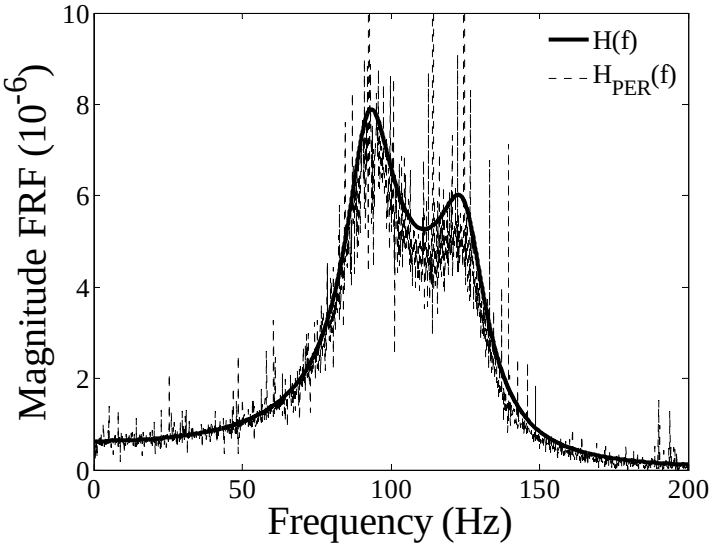

Figure 1: The analytically calculated FRF and a single periodogram estimate of the magnitude FRF $H_{12}(f)$.

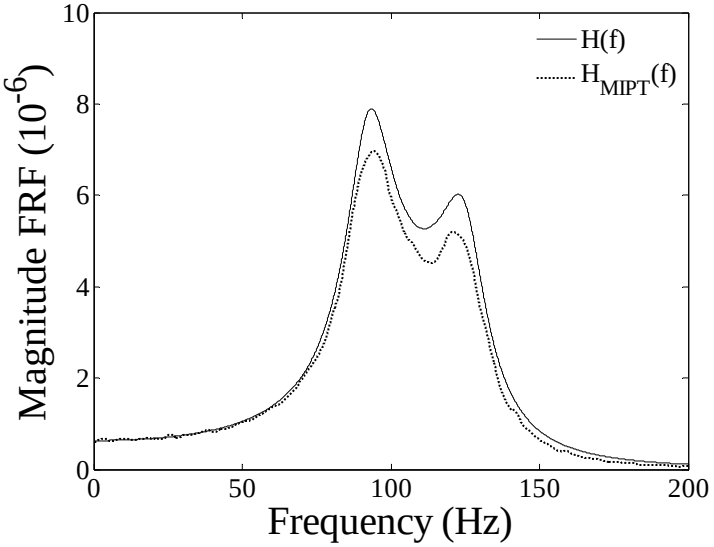

Figure 2: The analytically calculated FRF and the MIPT denoised single periodogram estimate of the magnitude FRF $H_{12}(f)$.

In a series of FRF estimates, the averaged periodogram is compared to the averages of the MIPT denoised FRFs in figure 3. It is evident that the MIPT denoised periodograms converge much faster than the regular periodogram, requiring less than 10 averages in this case.

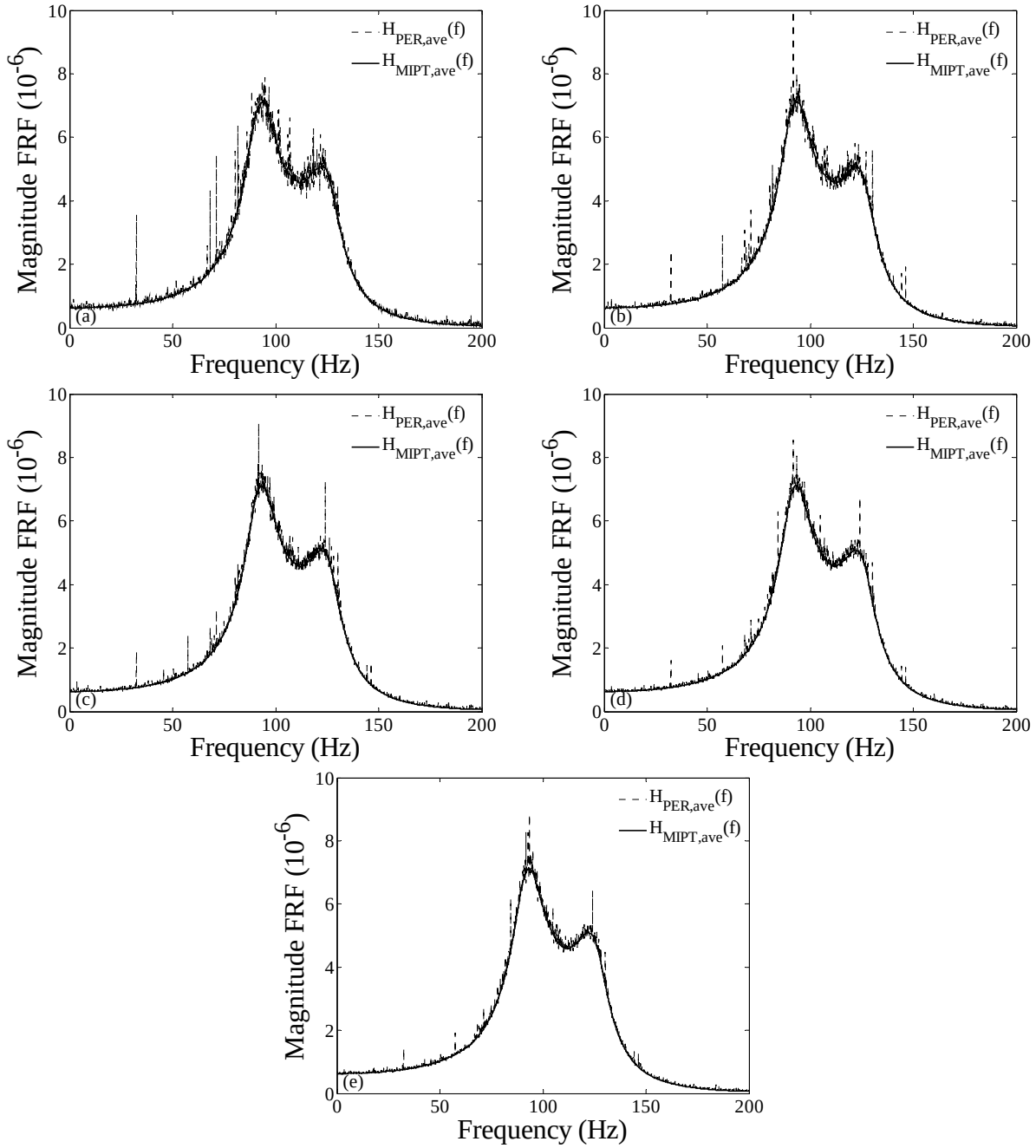

Figure 3: The improvement in periodogram estimates through averaging with and without MIPT denoising for the magnitude FRF $H_{12}(f)$ (a) 10 averages, (b) 20 averages, (c) 30 averages, (d) 40 averages, (e) 50 averages.

4 CONCLUSIONS AND FUTURE WORK

Experimentally obtained FRF estimates suffer from estimation variance and noise contamination. The SαS distribution is proposed to model FRF noise contamination. The validation of the SαS noise model is deferred to a future correspondence. In this paper, a MIPT based denoising algorithm is suggested to eliminate noise contamination in FRFs. The forward and inverse MIPT have the complexity $\mathcal{O}(N \log_3 N)$ and $\mathcal{O}(N)$, respectively.

Therefore, the MIPT is computationally more complex than the FFT. However, the MIPT noise reduction method can be implemented as a post processor to a periodogram based FRF estimator, considerably decreasing the variance on the final estimates and the time averages required. Furthermore, the MIPT involves repetitions of simple arithmetic operations (e.g., in the calculation of the polynomial coefficients) and can be implemented very efficiently in real-time on a dedicated processor. While the MIPT based algorithm is very effective in reducing estimation variance, its improvement capability is limited for estimation biases. To follow up the work presented in this paper, the MIPT based denoising algorithm will be tested on experimental vibration data. In addition, possible improvements in the noise reduction performance of the MIPT based algorithm through evaluation of the optimal threshold and decomposition levels will be investigated in future publications.

5 REFERENCES

[1] William J. Palm III, *System Dynamics*, (McGraw-Hill, New York, 2005).

[2] Alan V. Oppenheim, Ronald W. Schafer and John R. Buck, *Discrete-Time Signal Processing*, (Pearson Education, Singapore, 1999).

[3] Steven M. Kay, *Modern Spectral Estimation: Theory and Applications* (Prentice-Hall, Upper Saddle River, New Jersey, 1988).

[4] David L. Donoho, "De-noising by soft-thresholding," IEEE Transactions on Information Theory, **41**(3), 613-627 (1995).

[5] Agostino Abbate, Casimer DeCusatis and Pankaj K. Das, *Wavelets and Subbands: Fundamentals and Applications*, (Birkhäuser, New York, 2002).

[6] Per Bodin and Bo Wahlberg, "A frequency response estimation method based on smoothing and thresholding," International Journal of Adaptive Control and Signal Processing, **12**, 407-416 (1998).

[7] Y. Y. Kim, J.-C. Hong and N.-Y. Lee, "Frequency response functions estimation via a robust wavelet de-noising method," Journal of Sound and Vibration, **244**(4), 635-649 (2001).

[8] A. G. Bruce, David L. Donoho, Hong-Ye Gao and R. Douglas Martin, "Denoising and robust non-linear wavelet analysis," *Proceedings of SPIE Conference* (1994), pp. 325-336.

[9] David L. Donoho and Thomas P.-Y. Yu, "Robust nonlinear wavelet transform based on median-interpolation," *ASILOMAR Conference on Signals, Systems & Computers* (1997), pp. 75-79.

[10] David L. Donoho and Thomas P.-Y. Yu, "Nonlinear pyramid transforms based on median-interpolation," SIAM Journal on Mathematical Analysis, **31**(5), 1030-1061 (2000).

[11] Chrysostomos L. Nikias and Min Shao, *Signal Processing with Alpha-Stable Distributions and Applications*, (John Wiley, New York, 1995).